

Data Selection: A General Principle for Building Small Interpretable Models

Abhishek Ghose^a

Abstract. We present convincing empirical evidence for an effective and general strategy for building accurate small models. Such models are attractive for interpretability and also find use in resource-constrained environments. The strategy is to *learn* the training distribution and sample accordingly from the provided training data. The distribution learning algorithm is not a contribution of this work; our contribution is a rigorous demonstration of the broad utility of this strategy in various practical settings. We apply it to the tasks of (1) building cluster explanation trees, (2) prototype-based classification, and (3) classification using Random Forests, and show that *it improves the accuracy of decades-old weak traditional baselines to be competitive with specialized modern techniques.*

This strategy is also versatile wrt the notion of model size. In the first two tasks, model size is considered to be number of leaves in the tree and the number of prototypes respectively. In the final task involving Random Forests, the strategy is shown to be effective even when model size comprises of more than one factor: number of trees and their maximum depth.

Positive results using multiple datasets are presented that are shown to be statistically significant.

1 Introduction

The application of Machine Learning to various domains often leads to specialized requirements. One such requirement is small model size, which is useful in the following scenarios:

1. **Interpretability:** It is easier for humans to parse models when they are small. For example, a decision tree with a depth of 5 is likely easier to understand than one with a depth of 50. Multiple user studies have established model size as an important factor for interpretability [12, 27, 36]. This is also true for *explanations* that are models, where *post-hoc* interpretability is desired, e.g., local linear models with a small number of non-zero coefficients as in *LIME* [37] or *cluster explanation trees* with a small number of leaves [31, 26].
2. **Resource-constrained devices:** Small models are preferred when the compute environment is limited in various ways, such as memory and power [38, 19, 32]. Examples of such environments are micro-controllers, embedded devices and edge devices.

Of course, in these cases, we also prefer that small models do not drastically sacrifice predictive power. Typically this trade-off between size and accuracy is controlled in a manner that is specific to a model's formulation, e.g., $L1$ regularization for linear models, early stopping for Decision Trees. However, in this work we highlight a

universal strategy: *learn the training distribution*. This can often increase accuracy of small models, and thus addresses this trade-off in a model-agnostic manner. This was originally demonstrated in Ghose and Ravindran [17, 18]. Our work significantly extends the empirical evidence to show that such a strategy is indeed general and effective, and presents new evidence to show that it is also competitive.

1.1 Motivation and Contributions

We empirically show that the strategy of learning the training distribution improves accuracy of small models in diverse setups. Previous work that proposed this technique [17, 18] demonstrate such improvements for a *given* model; however, they leave an important question unanswered: are these improvements significant enough to be comparable to *other* models *tailored* to a task? Why might we use this strategy instead of using a contemporary specialized technique? This is the practical gap this work fills, where our answer is affirmative.

We consider the following tasks, for which we set ourselves the goal of constructing easy-to-interpret models:

1. Building cluster explanation trees.
2. Prototype-based classification.
3. Classification using Random Forests (RF).

For evaluation on each of these tasks, we follow a common theme: (a) first, we show that a traditional technique is almost always not as good as newer and specialized techniques, and, (b) then we show that its performance may be radically improved by learning the training distribution. Collectively, these evaluations show that the strategy of learning the training distribution is both *general* - may be applied to different tasks, models, notions of model sizes - and *effective* - results in competitive performance. These rigorous evaluations in diverse practical setups is the primary contribution of this work.

Table 1 concisely presents our setup and (one set of) observations. It lists various techniques compared on a task, including the traditional technique whose performance we seek to improve (highlighted in **red**), and the task-specific notion of model size (in **blue**). For all evaluations multiple trials are run (per dataset and model size combination; the datasets are also listed), and tests for statistical significance are conducted. The p -value of the improvement in prediction accuracy (based on a *Wilcoxon signed-rank test*) - of the traditional model using the provided training data vs using sampled data based on a learned distribution - is shown in the last column (smaller numbers are better). The general setup is further detailed in Section 4.

Table 1. Experiments at a glance. The methods that are **highlighted in red** were augmented with training distribution learning in our experiments. The year in which a method was proposed is also mentioned. Notably, this strategy improves relatively old methods to be at par with newer specialized techniques for varied notions of model size. What “model size” means for a task is **specified in blue**. The p -value from a statistical test comparing the original and augmented models appears in the last column; smaller is better.

Task	Methods	Metric	Significance Tests	Datasets	p -value of improvements (smaller is better)
(1) Explainable Clustering size = # leaves in a tree Section 5	Iterative Mistake Minimization (2020), ExShallow (2021), CART (1984)	Cost Ratio (ratio of F1 scores)	Friedman, Wilcoxon	(1) avila, (2) Sensorless, (3) covtype.binary, (4) covtype, (5) mice-protein	$p = 1.4783 \times 10^{-6}$
(2) Prototype-based Classification size = # prototypes Section 6	ProtoNN (2017), Stochastic Neighbor Compression (2014), Fast Condensed Nearest Neighbor Rule (2005) RBF Network (1988)	F1-macro	Friedman, Wilcoxon	(1) adult, (2) covtype.binary, (3) senseit-sei, (4) senseit-aco (5) phishing	$p = 1.699 \times 10^{-4}$
(3) Classification using Random Forests size = {tree depth, # trees} Section 7	Optimal Tree Ensemble (2020), subforest-by-prediction (2009), Random Forest (2001)	F1-macro	Friedman, Wilcoxon	(1) Sensorless, (2) heart, (3) covtype, (4) breast cancer, (5) ionosphere	$p = 1.44 \times 10^{-11}$

1.2 Organization

This is conceptually a short paper, i.e., has a simple well-defined central thesis, and is predominantly an empirical paper, i.e., the thesis is validated using experiments. We begin with a discussion of prior work (Section 2), followed by a brief overview of the technique we use to learn the training distribution (Section 3). The latter provides relevant context for our experiments. Critical to this paper is our measurement methodology - this is described in Section 4. The tasks mentioned in Table 1 are respectively detailed in Sections 5, 6 and 7. We summarize various results and discuss future work in the Section 8, which concludes the paper.

2 Previous Work

As mentioned, the only works we are aware of that discuss learning of the training distribution as a means to construct small models are Ghose and Ravindran [17, 18]. They propose techniques that maybe seen as forms of “adaptive sampling”: parameters for the training distribution are iteratively learned by adapting them to maximize held-out accuracy. In the rest of this paper, we will refer to these techniques as “Compaction by Adaptive Sampling” (COAS).

3 Overview of COAS

COAS iteratively learns the parameters of a training distribution based on performance on a held-out subset of the data, given a training algorithm, desired model size η and an accuracy metric of interest. It uses *Bayesian Optimization (BO)* [39] for its iterative learning. This specific optimizer choice allows for models with non-differentiable losses, e.g., decision trees. The output of one run of COAS is a *sample* of the training data drawn according to the learned distribution. For our experiments, the following hyperparameters of COAS are relevant:

1. Optimization budget, T : this is the number of iterations for which the optimizer runs. There is no other stopping criteria.
2. The lower and upper bounds for the size of the sample to be returned. This sample size is denoted by N_s .

Reasonable defaults exist for other hyperparameters [17]. We use the reference library *compactem* [16] in our experiments. A detailed review of COAS appears in Section A.1 of the Appendix.

4 Measurement

While each task-specific section contains a detailed discussion on the experiment setup, we discuss some common aspects here:

1. To compare model families $\mathcal{F}_1, \mathcal{F}_2, \mathcal{F}_3$, each of which is, say, used to construct models for different sizes $\eta \in \{2, 3\}$, for datasets D_1, D_2, D_3 , we use the *mean rank*, and support our conclusions with statistical tests such as the *Friedman* [14] and *Wilcoxon signed-rank* [40] tests¹.

Typically mean rank is used to compare model families based on their accuracies across datasets - which, ignoring model sizes, may be visualized as a 3×3 table here, with rows representing datasets, and columns denoting model families - see Figure 1(a). An entry such as “ D_2, \mathcal{F}_3 ” represents the accuracy (or some other metric) of a model from family \mathcal{F}_3 on dataset D_2 . Models are ranked on a per-dataset basis, i.e., row-wise, and the average ranks (computed per family, i.e., column-wise) are reported (lower is better). For statistical tests, the column values are directly used.

However, we have an additional factor here - the model size. To avoid inventing a custom metric, we assimilate it in the previous scheme by using the combination of datasets *and* model sizes as a row - see Figure 1(b). We think of such combinations as “pseudo-dataset” entries, i.e., now we have a 6×3 table, with rows for $D_1^2, D_1^3, D_2^2, D_2^3, D_3^2, D_3^3$, and same columns as before. The entry for “ D_1^2, \mathcal{F}_3 ” indicates the accuracy of a model of size 2 from family \mathcal{F}_3 on dataset D_1 .

Effectively, now the comparisons automatically account for model size since we use pseudo-datasets instead of datasets. **Note** that no new datasets are being created - we are merely defining a convention to include model size in the familiar dataset-model cross-product table.

2. For *each* model family, model size and dataset combination (essentially a cell in this cross-product table), models are constructed multiple times (we refer to these as multiple “trials”), and their scores are averaged. For tasks #1 and #2, five trials were used, whereas for task #3, three trials were used.
3. Key results for tasks #1, #2 and #3 appear in Sections 5.3, 6.3 and 7.3 respectively.

¹ The *Wilcoxon signed-rank* test was used here since it has been advocated by various studies for measuring classification performance [9, 3, 21].

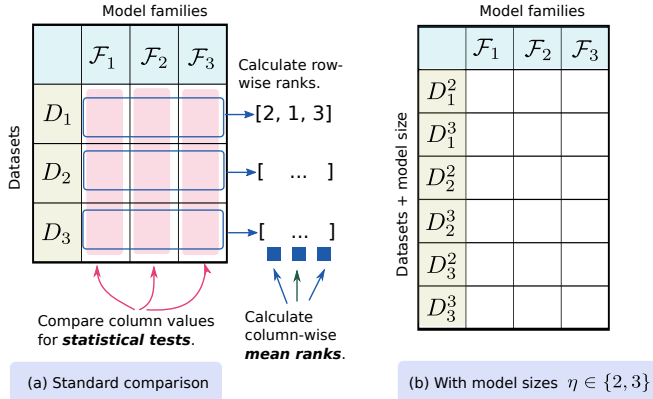


Figure 1. (a) shows a standard measurement scheme with datasets in rows and model families in columns. Statistical tests are performed on the column values. Row-wise ranks are first computed for calculating the mean rank. (b) To account for model sizes, we allow rows to represent combinations of datasets and model sizes. Details.

5 Explainable Clustering

The first task we investigate is the problem of *Explainable Clustering*. Introduced by [31], the goal is to explain cluster allocations as discovered by techniques such *k-means* or *k-medians*. This is achieved by constructing axis-aligned decision trees with leaves that either exactly correspond to clusters, e.g., *Iterative Mistake Minimization (IMM)* [31], or are proper subsets, e.g., *Expanding Explainable k-Means Clustering (ExKMC)* [15]. We consider the former case here, i.e., a tree must possess exactly k leaves to explain k clusters.

For a specific clustering C , let $C(x_i)$ denote the assigned cluster for an instance $x_i, i = 1 \dots N$, where $C(x_i) \in \{1, 2, \dots, k\}$, and the cluster centroids by $\mu_j, j = 1, \dots, k$. The cost of clustering J is then given by:

$$J = \frac{1}{N} \sum_{j=1}^k \sum_{\{x_i | C(x_i)=j\}} \|x_i - \mu_j\|_2^2 \quad (1)$$

In the case of an explanation trees with k leaves, μ_j are centroids of leaves. Cluster explanation techniques attempt to minimize this cost.

The price of explainability maybe measured as the *cost ratio*²:

$$\text{cost ratio} = \frac{J_{Ex}}{J_{KM}} \quad (2)$$

Here J_{Ex} is the cost achieved by an explanation tree, and J_{KM} is the cost obtained by a standard *k-means* algorithm. It assumes values in the range $[1, \infty]$, where the lowest cost is obtained when using *k-means*, i.e., J_{Ex} and J_{KM} are the same.

One may also indirectly minimize the cost in the following manner: use *k-means* to produce a clustering, use the cluster allocations of instances as their labels, and then learn a standard decision tree for classification, e.g., *CART*. This approach has been shown to be often outperformed by tree construction algorithms that directly minimize the cost in Equation 1, e.g., *IMM*.

5.1 Algorithms and Hyperparameters

The algorithms we compare and their hyperparameter settings are as follows:

² This is referred to as the *cost ratio* in Frost et al. [15], *price of explainability* in Moshkovitz et al. [31] and *competitive ratio* in Makarychev and Shan [30].

1. **Iterative Mistake Minimization (IMM)** [31]: This generates a decision tree via greedy partitioning using a criterion that minimizes number of mistakes at each split (the number of points separated from their corresponding reference cluster center). There are no parameters to tune. We used the implementation available here: <https://github.com/navefr/ExKMC>, which internally uses the reference implementation for IMM.
2. **ExShallow** [26]: Here, the decision tree construction explicitly accounts for minimizing explanation complexity while targeting a low cost ratio. The trade-off between clustering cost and explanation size is controlled via a parameter λ . This is set as $\lambda = 0.03$ in our experiments; this value is used in the original paper for various experiments. We used the reference implementation available here: <https://github.com/lmurtinho/ShallowTree>.
3. **CART w/o COAS**: We use *CART* [6] as the traditional model to compare, and maximize the classification accuracy for predicting clusters, as measured by the F1-macro score. The implementation in *scikit* [35] is used. During training, we set the following parameters: (a) the maximum number of leaves (this represents *model size* η here) is set to the number of clusters k , and (b) the parameter *class_weight* is set to “*balanced*” for robustness to disparate cluster sizes. Results for *CART* are denoted with label **CART**. We then apply *COAS* to *CART*; these results are denoted as **c_CART**. We set $T = 2000$, and use default settings for other parameters, e.g., $N_s \in [400, |X_{train}|]$. Since we are explaining clusters (and not predicting on unseen data), the training, validation and test sets are identical.

5.2 Experiment Setup

The comparison is performed over five datasets (limited to 1000 instances), and for each dataset, $k = 2, 3, \dots, 10$ clusters are produced. Results for the cost ratio (Equation 2) are reported over *five* trials. Evaluations are performed over the following publicly available datasets: *avila*, *covtype*, *covtype.binary*, *Sensorless* [8] and *mice-protein* [11]. We *specifically picked* these datasets since *CART* is known to perform poorly on them [15, 26], and thus these provide a good opportunity to showcase the power of this strategy.

5.3 Observations

Figure 2 presents our results. Figure 2(a) shows the plot for the *mice-protein* dataset: the 95% confidence interval, in addition to cost ratio, is shown³. Plots for other datasets are shown miniaturized - (b), (c), (d), (e) in the interest of space. The cost for *k-means* is shown for reference a blue horizontal line at $y = 1$. Figure 2(f) shows the *mean ranks* of the various techniques (lower is better) across datasets and number of clusters (as described in Section 4, trials scores are averaged), and its title shows the $p\text{-value} = 6.688 \times 10^{-6}$ of a *Friedman test* conducted over the *top three techniques*: we restrict the test to top candidates since otherwise it would be very easy to obtain a low score favorable to us, due to the high cost ratios for *CART*. The low score indicates with high confidence that *ExShallow*, *IMM* and *c_CART* do not produce the same outcomes.

From the plot of mean ranks in Figure 2(f), we observe that although *CART* performs quite poorly, the application of *COAS* drastically improves its performance, to the extent that it competes favorably with techniques like *IMM* and *ExShallow*; its mean rank places

³ It might come as a surprise that the cost ratio increases with increasing k , but this seems to be a transient phenomenon; at even higher values of k we do observe that cost ratios collectively decrease. See Section A.2, Appendix.

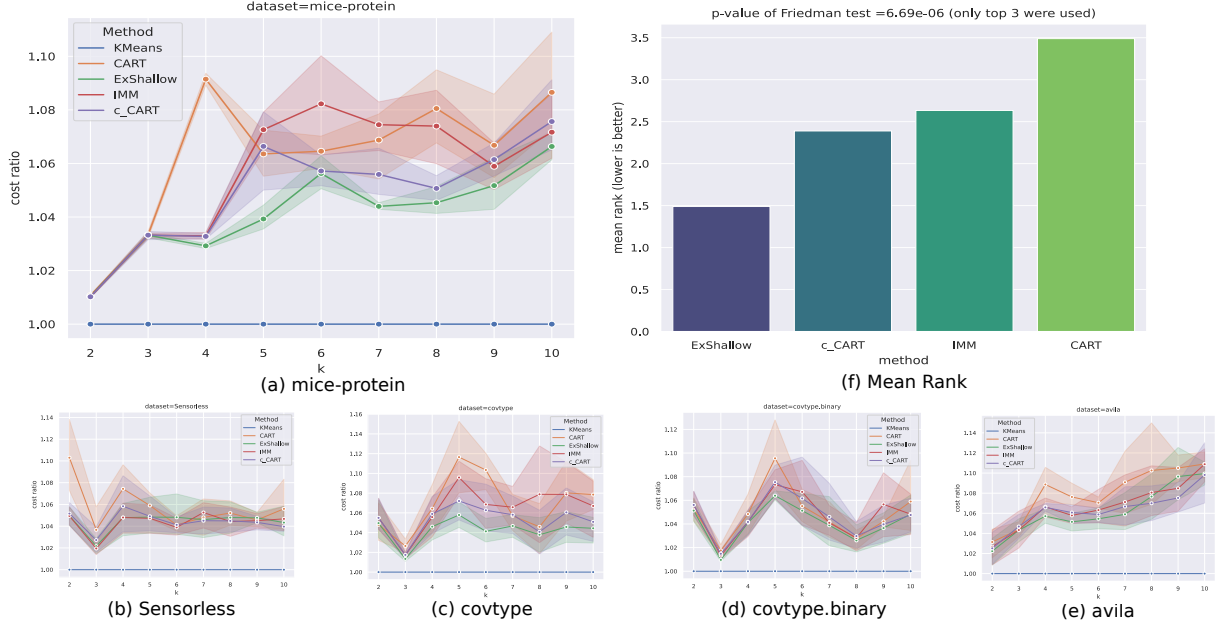


Figure 2. Comparisons over explainable clustering algorithms are shown. (a) shows the comparison for a specific dataset *mice-protein*. (b), (c), (d) and (e) show comparisons over other datasets - miniaturized to fit the page. (f) shows mean ranks of these techniques over five datasets across model sizes; the Friedman test is conducted over the **top three** techniques only, with $p = 6.688 \times 10^{-6}$.

it between them. This is especially surprising given that it doesn't explicitly minimize the cost in Equation 1. We also note the following *p-values* from *Wilcoxon signed-rank* tests:

- CART vs c_CART: $p = 1.4783 \times 10^{-6}$. The low value indicates that using COAS indeed significantly changes the accuracy of CART.
- IMM vs c_CART: $p = 0.0155$. The relatively high value indicates that the performance of c_CART is competitive with IMM.

Here, both the Friedman and Wilcoxon tests are performed for combinations of datasets and k - a "pseudo-dataset", as discussed in Section 4.

6 Prototype-based Classification

Next, we consider prototype-based classification. At training time, such techniques identify "prototypes" (actual training instances or generated instances), that maybe used to classify a test instance based on their similarity to them. A popular technique in this family is the *k-Nearest Neighbor (kNN)*. These are simple to interpret, and if a small but effective set of prototypes maybe identified, they can be convenient to deploy on edge devices [19, 42]. Prototypes also serve as minimal "look-alike" examples for explaining models [28, 33]. Research in this area has focused on minimizing the number of prototypes that need to be retained while minimally trading off accuracy.

We define some notation first. The number of prototypes we want is an input to our experiments, and is denoted by N_p . We will also use $K_\gamma(x_i, x_j) = e^{-\gamma \|x_i - x_j\|_2^2}$ to denote the *Radial Basis Function (RBF) kernel*, parameterized by the kernel bandwidth γ .

6.1 Algorithms and Hyperparameters

These are the algorithms we compare:

1. **ProtoNN** [19]: This technique uses a RBF kernel to aggregate influence of prototypes. Synthetic prototypes are learned and additionally a "score" is learned for each of them that designates their contribution towards *each* class. The prediction function sums the influence of neighbors using the RBF kernel, weighing contribution towards each class using the learned score values; the class with the highest total score is predicted. The method also allows for reducing dimensionality, but we don't use this aspect⁴. The various parameters are learned via gradient based optimization. We use the *EdgeML* library [10], which contains the reference implementation for ProtoNN. For optimization, the implementation uses the version of *ADAM* [24] implemented in *TensorFlow* [1]; we set $num_epochs = 200$, $learning_rate = 0.05$, while using the defaults for other parameters. The num_epochs and $learning_rate$ values are picked based on a limited search among values $\{100, 200, 300\}$ and $\{0.01, 0.05\}$ respectively. The search space explored for γ is $[0.001, 0.01, 0.1, 1, 10]$. Defaults are used for the other ProtoNN hyperparameters.
2. **Stochastic Neighbor Compression (SNC)** [25]: This also uses a RBF kernel to aggregate influence of prototypes, but unlike ProtoNN, the prediction is performed via the *1-NN rule*, i.e., prediction uses only the nearest prototype. The technique bootstraps with randomly sampled N_p prototypes (and corresponding labels) from the training data, and then modifies their coordinates for greater accuracy using gradient based optimization; the labels of the prototypes stay unchanged in this process. This is another difference compared to ProtoNN, where in the latter, each prototype contributes to all labels to varying extents. The technique maybe extended to reduce the dimensionality of the data (and prototypes); we don't use this aspect.

⁴ The implementation provides no way to switch off learning a projection, so we set the dimensionality of the projection to be equal to the original number of dimensions. This setting might however learn a transformation of the data to space within the same number of dimensions, e.g., translation, rotation.

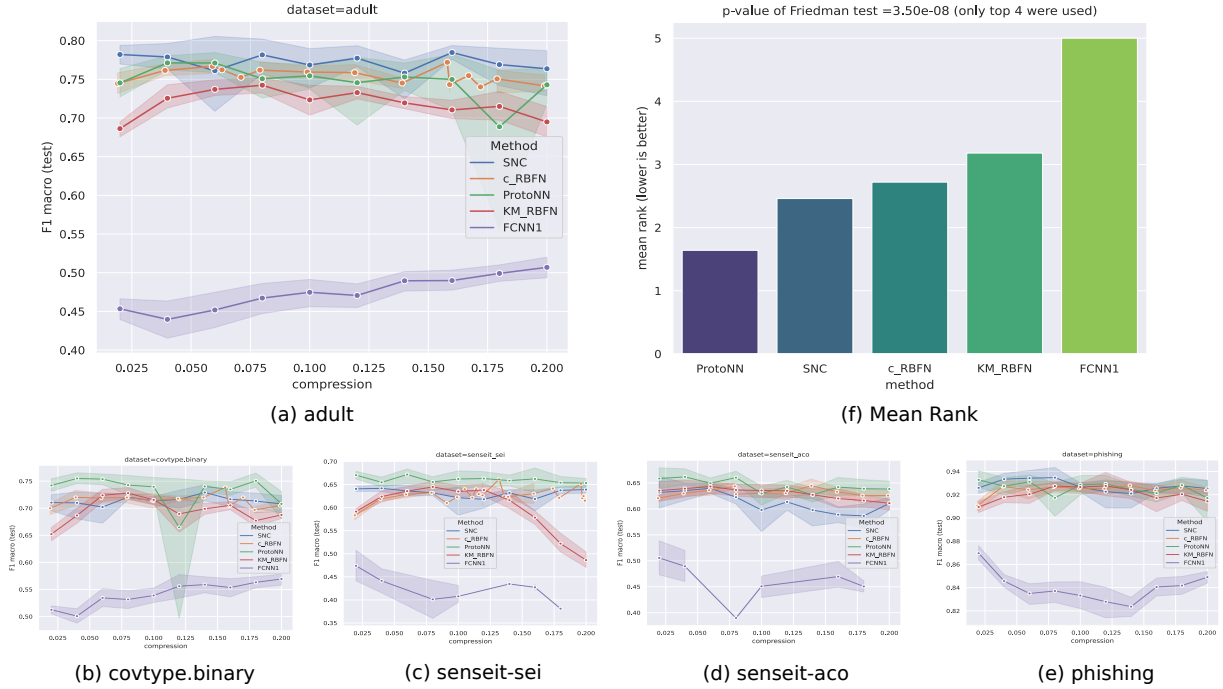


Figure 3. Various prototype-based classifiers are compared. (a) shows comparison for the dataset *adult*. Number of prototypes are shown as percentage of the training data on the *x*-axis, and is referred to as “compression”. (b), (c), (d) and (e) shows plots for other datasets - these are miniaturized to fit the page. (f) shows the mean ranks of techniques based on five datasets; the Friedman test is conducted over the **top four** techniques only, with $p = 3.5025 \times 10^{-8}$.

We were unable to locate the reference implementation mentioned in the paper, so we implemented our own version, with the help of the *JAXopt* library [4]. For optimization, gradient descent with *backtracking line search* is used. A total of 100 iterations for the gradient search is used (based on a limited search among these values: $\{100, 200, 300\}$), and each backtracking search is allowed up to 50 iterations. A grid search over the following values of γ is performed: $[0.001, 0.01, 0.1, 1, 10]$.

- Fast Condensed Nearest Neighbor Rule** [2]: Learns a “consistent subset” for the training data: a subset such that for any point in the training set (say with label l), the closest point in this subset also has a label l . Of the multiple variations of this technique proposed in [2], we use **FCNN1**, which uses the *1-NN* rule for prediction. There are no parameters to tune. We used our own implementation.

A challenge in benchmarking this technique is it *does not* accept N_p as a parameter; instead it iteratively produces expanding subsets of prototypes until a stopping criteria is met, e.g., if prototype subsets V_i and V_{i+1} are produced at iterations i and $i + 1$ respectively, then they satisfy the relationship $V_i \subset V_{i+1}$. For comparison, we consider the performance at iteration i to be the result of N_p prototypes where N_p is defined to be $|V_i|$, i.e., instead of setting N_p , we use the value the algorithm produces at each iteration.

- RBFN w/wo COAS**: For the traditional model, we use *Radial Basis Function Networks (RBFN)* [7]. For a binary classification problem with classes $\{-1, 1\}$, given prototypes $x_i, i = 1, 2, \dots, p$, the label of a test instance x is predicted as $\text{sgn}(\sum_i^p w_i K_\gamma(x, x_i))$ (a score of 0 is set to a label of 1). Weights w_i are learned using linear regression. A one-vs-rest setup is used for multiclass problems. For our baseline, we use cluster centres of a *k-means* clustering as our prototypes, where k is set to N_p . These results are denoted using the term **KM_RBFN**. In the COAS version, denoted by **c_RBFN**, the N_p prototypes are sampled from

the training data. N_p represents *model size* η here.

Note that the standard RBFN, and therefore the variants used here **KM_RBFN** and **c_RBFN**, don’t provide a way to reduce dimensionality; this is the reason why this aspect of ProtoNN and SNC wasn’t used (for fair comparison).

For COAS, we set $T = 1000$ and N_s was set to $[N_p - 1, N_p]$ to get the desired number of prototypes⁵.

Although all the above techniques use prototypes for classification, it is interesting to note variations in their design: ProtoNN, SNC, KM_RBFN use synthetic prototypes, i.e., they are not part of the training data, while c_RBFN and FCNN1 select N_p instances from the training data. The prediction logic also differs: ProtoNN, KM_RBFN, c_RBFN derive a label from some function of the influence by all prototypes, while SNC and FCNN1 use the 1-NN rule.

6.2 Experiment Setup

As before, we evaluate these techniques over five standard datasets: *adult*, *covtype.binary*, *senseit-sei*, *senseit-aco*, *phishing* [8]. 1000 training points are used, with $N_p \in \{20, 40, 60, 80, 100, 140, 160, 180, 200\}$. Results are reported over five trials. The score reported is the F1-macro score.

6.3 Observations

Results are shown in Figure 3. (a) shows the plot for the *adult* dataset. The number of prototypes are shown on the *x*-axis as *percentages* of the training data. Plots for other datasets are shown in (b), (c), (d) and (e); these have been miniaturized to fit the page. Figure 3(f) shows the mean rank (lower is better) across datasets and number of prototypes

⁵ The implementation [16] doesn’t allow for identical lower and upper bounds, hence the lower bound here is $N_p - 1$.

(as described in Section 4, trials are aggregated over). The p-value of the Friedman test is reported, $p = 3.5025 \times 10^{-8}$. Here too, we do not consider the worst performing candidate, FCNN1 - so as to not bias the Friedman test in our favor.

We observe in Figure 3(f) that while both ProtoNN and SNC outperform c_RBFN, the performance of SNC and c_RBFN are close. We also observe that FCNN1 performs poorly; this matches the observations in Kusner et al. [25].

We also consider the following *p-values* from *Wilcoxon signed-rank* tests:

1. KM_RBFN vs c_RBFN: $p = 1.699 \times 10^{-4}$. The low value indicates COAS significantly improves upon the baseline KM_RBFN.
2. SNC vs c_RBFN: $p = 0.1260$. The relatively high value here indicates that c_RBFN is competitive with SNC; in fact, at a confidence threshold of 0.1, their outcomes would not be interpreted as significantly different.

As discussed in Section 4, these statistical tests are conducted over a combination of dataset and model size.

7 Random Forest

In the previous sections, we considered the case of scalar model sizes: number of leaves in the case of explanation trees for clustering (Section 5) and number of prototypes in the case of prototype-based classification (Section 6). Here, we assess the effectiveness of the technique when the model size is composed of multiple factors.

We look at the case of learning *Random Forests (RF)* where we specify model size using *both* the number of trees and the maximum depth per tree.

7.1 Algorithms and Hyperparameters

The algorithms compared are:

1. **Optimal Tree Ensembles (OTE)** [23]: This is a technique to *prune* a RF to produce a lower number of trees. The pruning occurs in two phases: (a) first, the top M trees are retained based on prediction accuracy on *out-of-bag* examples, and (b) further pruning is performed based on a tree’s contribution to the overall *Brier score* on a validation set. In our experiments, M was set to 20% of the initial number of trees in the forest. Although a reference R package exists [22], it doesn’t allow to set the max. depth of trees, which is relevant here. Hence we use our implementation.
2. **Finding a subforest** [41]: This paper proposes multiple techniques to prune the number of trees in an RF. Among them it shows that pruning based on incremental predictive power of trees performs best. Hence, this is the technique we use here, based on our own implementation.
3. **RF w/wo COAS**: We train standard RFs [5] without and with COAS, denoted as **RF** and **c_RF** respectively. For COAS, we set number of iterations as $T = 3000$ and $N_s \in [30, |X_{train}|]$ (the lower bound was obtained by limited search). The implementation in *scikit* is used, and for standard RF models, i.e., without COAS, the parameter *class_weight* is set to “*balanced_subsample*” to make them robust to class imbalance.

7.2 Experiment Setup

We use the following five standard datasets for this experiment: *heart*, *Sensorless*, *covtype*, *ionosphere*, *breast cancer* [8]. For each

dataset, all size combinations from the following sets are tested (three trials per combination): $num_trees \in \{2, 5, 7, 10\}$ and $max_depth \in \{1, 2, 5, 7\}$. The total dataset size used had 3250 instances, with 70 : 30 split for train to test. For both OTE and the subforest-finding technique, the RFs were originally constructed with 100 trees, which were then pruned to the desired number. We report the F1-macro score in our experiments.

7.3 Observations

Figure 4(a) shows the results for dataset *Sensorless*; the *x-axis* shows values of the tuple (num_trees, max_depth) sorted by the first and then the second index. Note the “sawtooth” pattern. For a given value of num_trees , increase in max_depth leads to increasing accuracy. However, as we move to the next value for num_trees , we start with $max_depth = 1$ again, which leads to a drop in accuracy. This is an artefact of the ordering of the *x-axis*, and is expected behavior. Plots for other datasets are shown in (b), (c), (d) , (e) - these are miniaturized in the interest of space. Figure 4(f) shows mean ranks across datasets, number of trees and maximum tree depths (across trials).

OTE results are discounted for the Friedman test on account of its relatively poor performance. This gives us a p-value of $p = 6.17 \times 10^{-22}$, denoting sufficiently different outcomes.

It is easy to see that c_RF is the best performing technique here. The *p-value* for *Wilcoxon signed-rank* test wrt the standard RF is $p = 1.44 \times 10^{-11}$, demonstrating significant improvement.

In the interest of fairness, **please note** that both OTE and subforest-finding, in their original papers *do not* restrict the max. depth of trees, and as such, their use here should be seen as a modification, and not indicative of their performance on the original intended use-cases.

8 Discussion and Future Work

We note that a different number of iterations, T , were used for the tasks - see Sections 5.1, 6.1 and 7.1. This is because there is no widely-accepted stopping criteria for BO (although it has been studied [29, 20]), and the task-specific values were arrived at by limited search.

The experiments here clearly showcase both the versatility and effectiveness of the strategy of learning the training distribution: it may be applied to different models and notions of model sizes, and *importantly*, it can produce results that are competitive with specialized techniques.

While not directly related, it is equally important for us to call out what we are *not* claiming. We don’t propose that COAS replace the techniques it was compared to without further study, as the latter may offer other task specific benefits, e.g., ExShallow targets other explanation-quality metrics aside from the cost ratio. COAS might be able to address these dimensions as well, but it is beyond the scope of this study. Another reason for caution is that the improvements of COAS diminish as model sizes increase [17] ; hence, its utility to a task depends on what model size range is acceptable.

Instead, this work is a call to action to explore the strategy of learning the training distribution to build small accurate models - which we believe is relatively unknown today.

In terms of future work, some directions are: (a) learn weights for training instances (as opposed to a distribution) using *bilevel optimization* [34, 13] for the case of a differentiable training loss function, (b) COAS itself may be improved with the use of a different

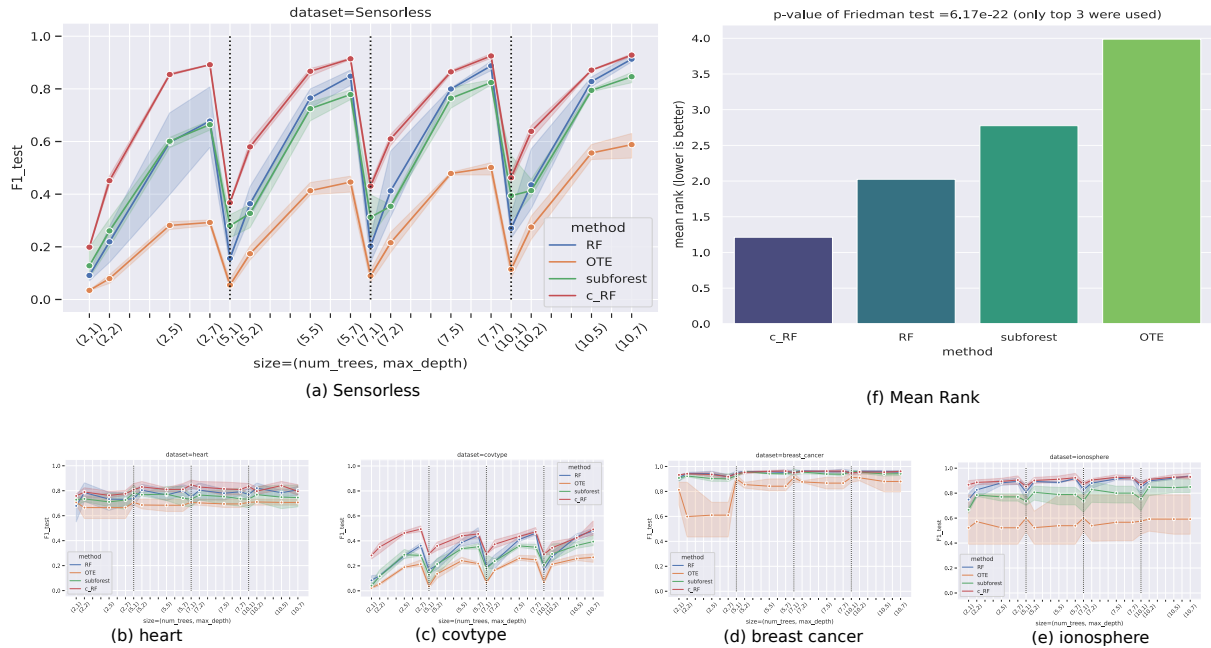


Figure 4. (a) shows results for the dataset=*covtype*. (b), (c), (d) and (e) show plots for other datasets - miniaturized to fit the page. (f) provides mean ranks, but since there are only two models being compared, the Friedman test cannot be performed.

black-box optimizer, and (c) develop a theoretical framework that explains this strategy.

References

- [1] M. Abadi, A. Agarwal, P. Barham, E. Brevdo, Z. Chen, C. Citro, G. S. Corrado, A. Davis, J. Dean, M. Devin, S. Ghemawat, I. Goodfellow, A. Harp, G. Irving, M. Isard, Y. Jia, R. Jozefowicz, L. Kaiser, M. Kudlur, J. Levenberg, D. Mané, R. Monga, S. Moore, D. Murray, C. Olah, M. Schuster, J. Shlens, B. Steiner, I. Sutskever, K. Talwar, P. Tucker, V. Vanhoucke, V. Vasudevan, F. Viégas, O. Vinyals, P. Warden, M. Wattenberg, M. Wicke, Y. Yu, and X. Zheng. TensorFlow: Large-scale machine learning on heterogeneous systems, 2015. URL <https://www.tensorflow.org/>. Software available from tensorflow.org.
- [2] F. Angiulli. Fast condensed nearest neighbor rule. In *Proceedings of the 22nd International Conference on Machine Learning, ICML '05*, page 25–32, New York, NY, USA, 2005. Association for Computing Machinery. ISBN 1595931805. doi: 10.1145/1102351.1102355. URL <https://doi.org/10.1145/1102351.1102355>.
- [3] A. Benavoli, G. Corani, and F. Mangili. Should we really use post-hoc tests based on mean-ranks? *Journal of Machine Learning Research*, 17(5):1–10, 2016. URL <http://jmlr.org/papers/v17/benavoli16a.html>.
- [4] M. Blondel, Q. Berthet, M. Cuturi, R. Frostig, S. Frostig, F. Linares-López, F. Pedregosa, and J.-P. Vert. Efficient and modular implicit differentiation. *arXiv preprint arXiv:2105.15183*, 2021.
- [5] L. Breiman. Random forests. *Machine Learning*, 45(1):5–32, Oct 2001. ISSN 1573-0565. doi: 10.1023/A:1010933404324. URL <https://doi.org/10.1023/A:1010933404324>.
- [6] L. Breiman et al. *Classification and Regression Trees*. Chapman & Hall, New York, 1984. ISBN 0-412-04841-8.
- [7] D. Broomhead and D. Lowe. Multivariable functional interpolation and adaptive networks. *Complex Systems*, 2:321–355, 1988.
- [8] C.-C. Chang and C.-J. Lin. LIBSVM: A library for support vector machines. *ACM Transactions on Intelligent Systems and Technology*, 2:27:1–27:27, 2011. Software available at <http://www.csie.ntu.edu.tw/~cjlin/libsvm>, datasets at <https://www.csie.ntu.edu.tw/~cjlin/libsvmtools/datasets/>.
- [9] J. Demšar. Statistical comparisons of classifiers over multiple data sets. *Journal of Machine Learning Research*, 7(1):1–30, 2006. URL <http://jmlr.org/papers/v7/demšar06a.html>.
- [10] D. K. Dennis, Y. Gaurkar, S. Gopinath, S. Goyal, C. Gupta, M. Jain, S. Jaiswal, A. Kumar, A. Kusupati, C. Lovett, S. G. Patil, O. Saha, and H. V. Simhadri. EdgeML: Machine Learning for resource-constrained edge devices, 2021. URL <https://github.com/Microsoft/EdgeML>.
- [11] D. Dua and C. Graff. UCI machine learning repository, 2017. URL <http://archive.ics.uci.edu/ml>.
- [12] J. Feldman. Minimization of boolean complexity in human concept learning. *Nature*, 407:630–3, 11 2000. doi: 10.1038/35036586.
- [13] L. Franceschi, P. Frasconi, S. Salzo, R. Grazi, and M. Pontil. Bilevel programming for hyperparameter optimization and meta-learning. In J. Dy and A. Krause, editors, *Proceedings of the 35th International Conference on Machine Learning*, pages 1568–1577. PMLR, 10–15 Jul 2018. URL <https://proceedings.mlr.press/v80/franceschi18a.html>.
- [14] M. Friedman. The use of ranks to avoid the assumption of normality implicit in the analysis of variance. *Journal of the American Statistical Association*, 32(200):675–701, 1937. ISSN 01621459. URL <http://www.jstor.org/stable/2279372>.
- [15] N. Frost, M. Moshkovitz, and C. Rashtchian. Exkmc: Expanding explainable k -means clustering. *arXiv preprint arXiv:2006.02399*, 2020.
- [16] A. Ghose. compactem, Nov. 2020. URL <https://pypi.org/project/compactem/>. Software available at <https://compactem.readthedocs.io/en/latest/index.html>.
- [17] A. Ghose and B. Ravindran. Learning interpretable models using an oracle. *CoRR*, abs/1906.06852, 2019. URL <http://arxiv.org/abs/1906.06852>.
- [18] A. Ghose and B. Ravindran. Interpretability with accurate small models. *Frontiers in Artificial Intelligence*, 3, 2020. ISSN 2624-8212. doi: 10.3389/frai.2020.00003. URL <https://www.frontiersin.org/articles/10.3389/frai.2020.00003>.
- [19] C. Gupta, A. S. Suggala, A. Goyal, H. V. Simhadri, B. Paranjape, A. Kumar, S. Goyal, R. Udupa, M. Varma, and P. Jain. ProtoNN: Compressed and accurate kNN for resource-scarce devices. In D. Precup and Y. W. Teh, editors, *Proceedings of the 34th International Conference on Machine Learning*, volume 70 of *Proceedings of Machine Learning Research*, pages 1331–1340. PMLR, 06–11 Aug 2017. URL <https://proceedings.mlr.press/v70/gupta17a.html>.
- [20] H. Ishibashi, M. Karasuyama, I. Takeuchi, and H. Hino. A stopping criterion for bayesian optimization by the gap of expected minimum simple regrets. In F. Ruiz, J. Dy, and J.-W. van de Meent, editors, *Proceedings of The 26th International Conference on Artificial Intelligence and Statistics*, volume 206 of *Proceedings of Machine Learning Research*, pages 6463–6497. PMLR, 25–27 Apr 2023. URL <https://proceedings.mlr.press/v206/ishibashi23a.html>.
- [21] N. Japkowicz and M. Shah. *Evaluating Learning Algorithms: A Classification Perspective*. Cambridge University Press, 2011. doi: 10.1017/CBO9780511921803.
- [22] Z. Khan, A. Gul, A. Perperoglou, O. Mahmoud, W. Adler, Miftahuddin, and B. Lausen. compactem, Apr. 2020. URL <https://cran.r-project.org/web/packages/OTE/>. Software available at <https://cran.r-project.org/web/packages/OTE/>.
- [23] Z. Khan, A. Gul, A. Perperoglou, M. Miftahuddin, O. Mahmoud,

- W. Adler, and B. Lausen. Ensemble of optimal trees, random forest and random projection ensemble classification. *Advances in Data Analysis and Classification*, 14(1):97–116, Mar 2020. ISSN 1862-5355. doi: 10.1007/s11634-019-00364-9. URL <https://doi.org/10.1007/s11634-019-00364-9>.
- [24] D. P. Kingma and J. Ba. Adam: A method for stochastic optimization. In Y. Bengio and Y. LeCun, editors, *3rd International Conference on Learning Representations, ICLR 2015, San Diego, CA, USA, May 7-9, 2015, Conference Track Proceedings*, 2015. URL <http://arxiv.org/abs/1412.6980>.
- [25] M. Kusner, S. Tyree, K. Weinberger, and K. Agrawal. Stochastic neighbor compression. In E. P. Xing and T. Jebara, editors, *Proceedings of the 31st International Conference on Machine Learning*, volume 32 of *Proceedings of Machine Learning Research*, pages 622–630, Beijing, China, 22–24 Jun 2014. PMLR. URL <https://proceedings.mlr.press/v32/kusner14.html>.
- [26] E. S. Laber, L. Murtinho, and F. Oliveira. Shallow decision trees for explainable k-means clustering. *CoRR*, abs/2112.14718, 2021. URL <https://arxiv.org/abs/2112.14718>.
- [27] I. Lage, E. Chen, J. He, M. Narayanan, B. Kim, S. J. Gershman, and F. Doshi-Velez. Human evaluation of models built for interpretability. *Proceedings of the AAAI Conference on Human Computation and Crowdsourcing*, 7(1):59–67, Oct. 2019. URL <https://ojs.aaai.org/index.php/HCOMP/article/view/5280>.
- [28] O. Li, H. Liu, C. Chen, and C. Rudin. Deep learning for case-based reasoning through prototypes: A neural network that explains its predictions. In *Proceedings of the Thirty-Second AAAI Conference on Artificial Intelligence and Thirtieth Innovative Applications of Artificial Intelligence Conference and Eighth AAAI Symposium on Educational Advances in Artificial Intelligence, AAAI’18/IAAI’18/EAAI’18*. AAAI Press, 2018. ISBN 978-1-57735-800-8.
- [29] A. Makarova, H. Shen, V. Perrone, A. Klein, J. B. Faddoul, A. Krause, M. Seeger, and C. Archambeau. Overfitting in bayesian optimization: An empirical study and early-stopping solution. In *ICLR 2021 Workshop on Neural Architecture Search*, 2021. URL <https://www.amazon.science/publications/overfitting-in-bayesian-optimization-an-empirical-study-and-early-stopping-solution>.
- [30] K. Makarychev and L. Shan. Explainable k-means: Don’t be greedy, plant bigger trees! In *Proceedings of the 54th Annual ACM SIGACT Symposium on Theory of Computing, STOC 2022*, page 1629–1642, New York, NY, USA, 2022. Association for Computing Machinery. ISBN 9781450392648. doi: 10.1145/3519935.3520056. URL <https://doi.org/10.1145/3519935.3520056>.
- [31] M. Moshkovitz, S. Dasgupta, C. Rashtchian, and N. Frost. Explainable k-means and k-medians clustering. In H. D. III and A. Singh, editors, *Proceedings of the 37th International Conference on Machine Learning*, volume 119 of *Proceedings of Machine Learning Research*, pages 7055–7065. PMLR, 13–18 Jul 2020. URL <https://proceedings.mlr.press/v119/moshkovitz20a.html>.
- [32] M. G. S. Murshed, C. Murphy, D. Hou, N. Khan, G. Ananthanarayanan, and F. Hussain. Machine learning at the network edge: A survey. *ACM Comput. Surv.*, 54(8), oct 2021. ISSN 0360-0300. doi: 10.1145/3469029. URL <https://doi.org/10.1145/3469029>.
- [33] M. Nauta, A. Jutte, J. Provoost, and C. Seifert. This looks like that, because ... explaining prototypes for interpretable image recognition. In M. Kamp, I. Koprinska, A. Bibal, T. Bouadi, B. Frénay, L. Galárraga, J. Oramas, L. Adilova, Y. Krishnamurthy, B. Kang, C. Largeton, J. Lijffijt, T. Viard, P. Welke, M. Ruocco, E. Aune, C. Gallicchio, G. Schiele, F. Pernkopf, M. Blott, H. Fröning, G. Schindler, R. Guidotti, A. Monreale, S. Rinzivillo, P. Biecek, E. Ntoutsi, M. Pechenizkiy, B. Rosenhahn, C. Buckley, D. Cialfi, P. Lanillos, M. Ramstead, T. Verbelen, P. M. Ferreira, G. Andresini, D. Malerba, I. Medeiros, P. Fournier-Viger, M. S. Nawaz, S. Ventura, M. Sun, M. Zhou, V. Bitetta, I. Bordino, A. Ferretti, F. Gullo, G. Ponti, L. Severini, R. Ribeiro, J. Gama, R. Gavaldà, L. Cooper, N. Ghazaleh, J. Richiardi, D. Roqueiro, D. Saldana Miranda, K. Sechidis, and G. Graça, editors, *Machine Learning and Principles and Practice of Knowledge Discovery in Databases*, pages 441–456, Cham, 2021. Springer International Publishing. ISBN 978-3-030-93736-2.
- [34] F. Pedregosa. Hyperparameter optimization with approximate gradient. In *Proceedings of the 33rd International Conference on International Conference on Machine Learning - Volume 48, ICML’16*, page 737–746. JMLR.org, 2016.
- [35] F. Pedregosa, G. Varoquaux, A. Gramfort, V. Michel, B. Thirion, O. Grisel, M. Blondel, P. Prettenhofer, R. Weiss, V. Dubourg, J. Vanderplas, A. Passos, D. Cournapeau, M. Brucher, M. Perrot, and E. Duchesnay. Scikit-learn: Machine learning in Python. *Journal of Machine Learning Research*, 12:2825–2830, 2011.
- [36] F. Poursabzi-Sangdeh, D. Goldstein, J. Hofman, J. Wortman Vaughan, and H. Wallach. Manipulating and measuring model interpretability. In *CHI 2021*, May 2021. URL <https://www.microsoft.com/en-us/research/publication/manipulating-and-measuring-model-interpretability/>.
- [37] M. T. Ribeiro, S. Singh, and C. Guestrin. “why should i trust you?”: Explaining the predictions of any classifier. In *Proceedings of the 22Nd ACM SIGKDD International Conference on Knowledge Discovery and Data Mining, KDD ’16*, pages 1135–1144, New York, NY, USA, 2016. ACM. ISBN 978-1-4503-4232-2. doi: 10.1145/2939672.2939778. URL <http://doi.acm.org/10.1145/2939672.2939778>.
- [38] R. Sanchez-Iborra and A. F. Skarmeta. Tinyml-enabled frugal smart objects: Challenges and opportunities. *IEEE Circuits and Systems Magazine*, 20(3):4–18, 2020. doi: 10.1109/MCAS.2020.3005467.
- [39] B. Shahriari, K. Swersky, Z. Wang, R. Adams, and N. De Freitas. Taking the human out of the loop: A review of bayesian optimization. *Proceedings of the IEEE*, 104(1):148–175, Jan. 2016. ISSN 0018-9219. doi: 10.1109/JPROC.2015.2494218. Publisher Copyright: © 1963-2012 IEEE.
- [40] F. Wilcoxon. Individual comparisons by ranking methods. *Biometrics Bulletin*, 1(6):80–83, 1945. ISSN 00994987. URL <http://www.jstor.org/stable/3001968>.
- [41] H. Zhang and M. Wang. Search for the smallest random forest. *Statistics and its interface*, 2:381, 01 2009. doi: 10.4310/SII.2009.v2.n3.a11.
- [42] W. Zhang, X. Chen, Y. Liu, and Q. Xi. A distributed storage and computation k-nearest neighbor algorithm based cloud-edge computing for cyber-physical-social systems. *IEEE Access*, 8:50118–50130, 2020. doi: 10.1109/ACCESS.2020.2974764.

A Appendix

A.1 Review of COAS

We briefly discuss COAS in this section. Specifically, we discuss the technique from Ghose and Ravindran [17]⁶. We simplify various aspects for brevity - for details please refer to the original paper.

We denote the *sampling process* used in COAS by $S((X, Y), \Psi, N_s, p_o)$. Here, (X, Y) is the data that is to be sampled from (*with replacement*) and Ψ, N_s, p_o are parameters used for sampling. These are defined as follows:

- Ψ : This is a *probability density function (pdf)* defined over the data⁷ (X, Y) and denotes the sampling probability of instances.
- N_s : Sample size.
- p_o : The fraction of samples that are to be sampled uniformly randomly from (X, Y) . The remaining $(1 - p_o)N_s$ samples are chosen with replacement from (X, Y) based on the probabilities $p((X, Y); \Psi)$.

p_o serves as a “shortcut” for the model to combine data that was provided with data from the learned distribution. Since the train and test data splits provided are assumed to come from the same distribution, p_o also acts as tool for analyzing the “mix” of data preferred at various model sizes. For example, an interesting result shown [17] is that as model size increases, $p_o \rightarrow 1$, i.e., the best training distribution at large sizes is the test distribution, which is the commonly known case.

To state the optimize problem COAS solves, we introduce additional notation:

1. Let (X_{train}, Y_{train}) and (X_{val}, Y_{val}) represent training and validation datasets respectively.
2. Let $train_{\mathcal{F}}(\eta, (X, Y))$ be a training algorithm that returns a model of size η from model family \mathcal{F} when supplied with training data (X, Y) .
3. Let $acc(f, (X, Y))$ denote the accuracy of model f on dataset (X, Y) .

Then, COAS performs the following optimization for user-specified η over T iterations:

$$\max_{\Psi, N_s, p_o} acc(f, (X_{val}, Y_{val})) \quad (3)$$

$$\text{where, } f = train_{\mathcal{F}}(\eta, (X_{sample}, Y_{sample})) \quad (4)$$

$$\text{and } (X_{sample}, Y_{sample}) = S((X_{train}, y_{train}), \Psi, N_s, p_o) \quad (5)$$

Essentially, COAS identifies parameters Ψ, N_s, p_o such that a model trained on data sampled using them, maximizes validation accuracy. Note that since $S()$ samples with replacement, it is possible to have an optimal N_s that’s larger than the size of the training data. A *Bayesian Optimizer* is used for optimization, and a *budget* of T iterations is provided. There is no other stopping criteria, i.e., the optimizer is run all the way through T iterations.

⁶ The techniques in the papers vary in terms of how they make the process of adaptive sampling tractable. In Ghose and Ravindran [18], a decision tree is used capture neighborhood information, which is then utilized for sampling. Ghose and Ravindran [17] uses the *prediction uncertainty* from an *oracle* model to aid sampling. The latter was shown to be more accurate in the respective paper, and this is why we use it here.

⁷ The *pdf* is applies to the data *indirectly*: it models the density of the prediction uncertainty scores of instances in (X, Y) , as provided by the oracle model. We use this simplification for brevity.

A.2 Cost Ratio Revisited

We had noted in Section 5.3 that cost ratios seem to increase with increasing k - consider the case of the `mice-protein` dataset in Figure 2(a). This is counter-intuitive since distances to centroids should decrease due to a finer partitioning of the space, which should drive down J_{Ex} in Equation 1. As shown in Figure 5, this indeed does happen after a temporary rise in cost-ratios; the figure shows the `mice-protein` dataset again, but now k goes up to 80 rather than 10 as in the main paper.

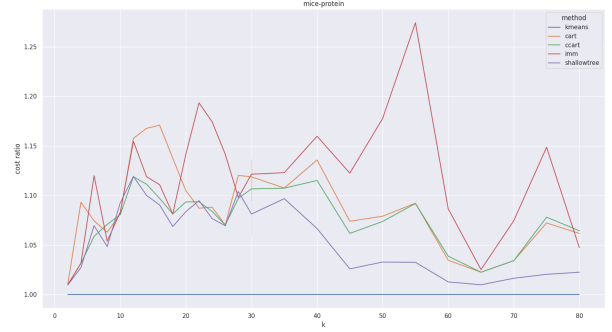


Figure 5. The cost ratio increases and then decreases with increasing k . Shown for the `mice-protein` dataset.